Calibration Models and Uncertainty Analysis of the Euroloop Liquid Hydrocarbon Flow Facility

Jos van der Grinten[1] and Bart van der Stap[2]

[1]*NMi EuroLoop, Petroleumweg 36, 3196 KD Rotterdam-Vondelingenplaat, The Netherlands*
[2]*Flowways, Eindhoven, The Netherlands*
E-mail corresponding author: jos.vandergrinten@nmi-euroloop.nl

Abstract

After initial experiences with the EuroLoop Liquid Hydrocarbon Flow Facility the initial uncertainty analysis was re-evaluated according to the GUM. Successive substitution was used to compute the deviation of a meter under test as a function of all input parameters. A number of uncertainty sources that requires specific attention are discussed.
Compared to the current accreditation the achievable CMC values are at least 30% lower for volumetric calibrations and 40% lower for mass flow calibrations. The reasons for the lower uncertainties are the utilization of the triple set of detectors in the piston prover, which results in three independent measurement results, and the stability of the measurement process that is better than originally anticipated. The CMC obtained for the big piston prover is 0.008%.

1. Introduction

Since the end of 2015 the EuroLoop Liquid Hydrocarbon Flow Facility is operated under accreditation [1]. With an increasing amount of operational experiences [2],[3] it is time to re-evaluate the initial uncertainty analysis. The objective of the analysis is to find the lowest uncertainty that is reasonably achievable for the test facility.

The primary references of the calibration facility are a 24" and a 48" piston prover, which were calibrated dimensionally by Dutch national standards laboratory VSL. Subsequently, the provers are used to calibrate the ultrasonic master meters in the system. In addition the provers can be used to calibrate a meter under test (MuT). The master meters can also used to calibrate the MuT, which can be a volume flow meter, a mass flow meter or a differential pressure device. The adjacent figure gives a schematic overview of the traceability.

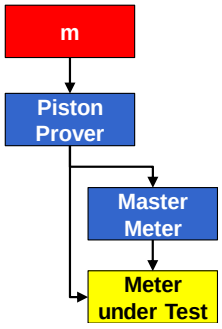

Figure 1: Schematic traceability chain

This paper gives an overview of the calibration models required for the uncertainty analysis of the volume calibration processes performed with the EuroLoop Liquid Hydrocarbon Flow Facility. These comprise the following calibrations.

a) Calibration of the master meters (MM) using a piston prover (PP).
b) Calibration of a Meter under Test (MuT) using a piston prover (PP).
c) Calibration of a Meter under Test (MuT) using a master meter (MM).

The processes described under item a) and b) use the same mathematical model-description. Obviously, there are different models for the calibration of volume and mass meters. The calibration facility consists of three independent calibration loops filled with a low, medium and high viscous product to cover a large Reynolds range. The uncertainty models are applicable for all liquid loops.

Throughout the paper the following generic assumptions are applicable for the uncertainty evaluation:

1. The flow during calibration activities is uniform and stationary (i.e. no pulsations, limited swirl at the MuT locations and temperature stabilized).
2. There is no leak or bypass flow in the pipe sections between the master meter, MuT and prover (if applicable).
3. The products have homogenous and uniform fluid properties and have no gaseous inclusions (i.e. bubble-free).

In the rest of the paper we will focus on the models used for the volumetric calibration models. The mass flow calibration models are similar but will not be shown in this paper.

2. Volumetric calibration model using master meters

The calibration of volume flow meters and mass flow meters with hydrocarbon liquids is based on the integral formulation of the mass conservation law applied to a fixed volume V with surface F. The increase in mass per unit time in V equals the mass flow through the surface F:

$$\frac{\partial}{\partial t}\iiint_V \rho \, dV = -\iint_F \rho \, (\mathbf{v}\cdot\mathbf{n}) \, dF \qquad (1)$$

in which $\mathbf{v}$ is the fluid velocity vector and $\mathbf{n}$ a normal vector of length 1 perpendicular to the surface F pointing outside of V. $(\mathbf{v}\cdot\mathbf{n})$ is the dot product of $\mathbf{v}$ and $\mathbf{n}$, which means that a fluid flow entering V gets a negative sign and a fluid flow leaving V gets a positive sign.

While calibrating, V is the volume between the master meters and the meter under test (MuT). The fluid enters V via the master meters and leaves V via the MuT. Both masters and MuT measure liquid in volume units. The volume V having thick steel walls is assumed to be constant in time. As the fluid flows through closed conduits, the fluid velocity times the cross section is the volume flow rate Q. Now equation (1) can be written as

$$V\frac{\partial \rho_V}{\partial t} = -\rho_2 Q_2 + \rho_1 Q_1 \qquad (2)$$

where the index 1 refers to the cross section at the master meter and 2 refers to the MuT. For entirely stationary conditions the left hand sid of Eq. (2) equals zero.

The density of the liquid ρ is a function of temperature t and the gauge pressure p

$$\rho = \rho_{15}\left(1-\gamma_l(t-t_{15})\right)\cdot(1+\kappa p) \qquad (3)$$

Where ρ_{15} is the liquid density at t_{15} (15°C), γ_l is the volume expansion coefficient and κ is the liquid compressibility. The volume expansion coefficient γ_l is obtained from density of a liquid sample analyzed over a range of temperatures by an independent accredited laboratory. The compressibility κ is obtained from ASTM tables.

The indicated flowrate Q is computed from an integer number of pulses N collected during an interval τ:

$$Q_s = \frac{N_s}{I_s\,\tau_s},\quad Q_m = \frac{N_m}{I_m\,\tau_m} \qquad (4)$$

in which I is the impulse factor of the meter [pulse/m³]. The objective of the calibration is to determine the deviation e_m of the meter under test as a function of the flowrate Q_m indicated by the MuT

$$e_m = \frac{Q_m}{Q_2} - 1 \qquad (5)$$

In the calibration process corrections are applied for all known deviations. For the master meter the deviation e_s is depending on the flowrate Q_s indicated by master. The correction for this deviation leads to

$$Q_1 = \frac{Q_s}{1+e_s} \qquad (6)$$

Due to the stable stationary conditions during calibration the accumulated mass, i.e. the dead volume correction for master meter calibrations will be treated as an uncertainty, which means that the left hand side of equation (2) is zero.
Successive substitution of equations (3-6) in equation (2) and solving the deviation e_m leads to:

$$e_m = \frac{\frac{\left(1-\gamma_l(t_m-t_{15})\right)\cdot(1+\kappa p_m)N_m}{I_m\,\tau_m}}{\frac{\left(1-\gamma_l(t_s-t_{15})\right)\cdot(1+\kappa p_s)\,N_s}{I_s\tau_s(1+e_s)}} - 1 \qquad (7)$$

3. Volumetric calibration model using piston provers

The piston prover is used to calibrate both the master meter and the meter under test, which can be performed simultaneously.

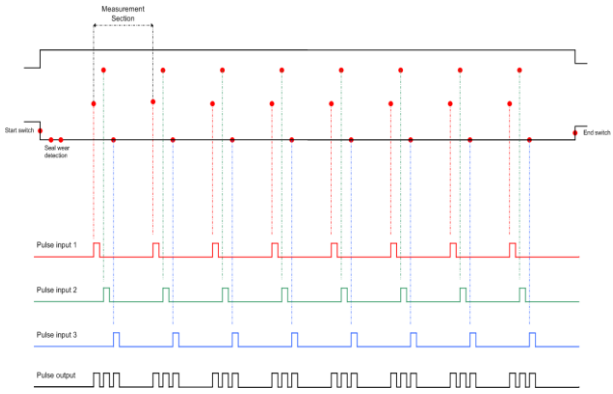

Figure 2: Measurement sections and sensor positions of the piston prover.

The prover is divided in sections with calibrated diameters and with known distances between the switches. As the prover is bi-directional, calibrations were performed moving the piston from north to south and from south to north. Each section has three switches j=1..3 located at the 2 o'clock, 4 o'clock and 8 o'clock positions when looking north. During calibration of the prover all actual dimensions were converted to dimensions at 20°C. The actual volume V_{ij} of prover section i between two j^{th} switches is calculated by:

$$V_{ij} = L_{20,ij}\cdot\left(1+\alpha_{st}(t_{wall}-t_{20})\right)\cdot \frac{\pi}{4}\cdot\left(D_{20,ij}\right)^2\cdot\left(1+2\alpha_{st}(t_{wall}-t_{20})\right)\cdot \left(1+\frac{p_{pp}D_{pp}}{Ew_{pp}}\right) \qquad (8)$$

As the diameter of the piston prover tube is much wider than the diameter of the pipework and the liquid velocities in the piston prover are much lower than the liquid velocities in the MuT, the pressure inside the piston prove is assumed to be constant.

Applying equation (2) for the prover setup, a cross-section could be defined as the cross section of the prover at the location of the prover end-switches. The fluid is moving with flow rate Q through this cross section, whereas the piston travels between the start and stop switches during the interval τ (i.e. the piston triggers the start and stop switches):

$$Q_{pp} = \frac{V_{ij}}{\tau_{pp,i,j}},\quad Q_m = \frac{N_m}{I_m\,\tau_m} \qquad (9)$$

in which I is the impulse-factor of the meter [pulse/m³].

On top of the generic assumptions the following conditions are applicable for piston proving:

1) The piston has a uniform motion inside the prover tube, which is monitored by measuring the flow variance while calibrating.

2) There is no fluid bypassing the piston seals during piston motion, validated by frequent leak tests.
3) The pressure and temperature measured at the prover cross section is representative of the pressure and temperature of the volume displaced by the piston.
4) The prover wall temperature is measured, shall be within 0.2°C equal to the product temperature, and shall be stable during calibration activities

As the prover volume determination already includes all known deviations, the flowrate Q_{pp} is defined as:

$$Q_1 = Q_{pp} \tag{10}$$

Successive substitution of Eqs (3, 5, 13 and 14) in Eq. (2) and solving the deviation e_m leads to:

$$e_{m,i,j} = \frac{\dfrac{\big(1-\gamma_l(t_m-t_{15})\big)\cdot(1+\kappa p_m)N_m}{I_m\,\tau_m}}{\dfrac{\big(1-\gamma_l(t_{pp}-t_{15})\big)\cdot(1+\kappa p_{pp})\,V_{i,j}}{\tau_{pp,i,j}}} - 1 \tag{11}$$

Substitution of Eq. (12) leads to a single expression for $e_{m,i,j}$ in which all variables are included:

$$e_{m,i,j} = \left(\frac{\big(1-\gamma_l(t_m-t_{15})\big)\cdot(1+\kappa p_m)N_m\tau_{pp,i,j}}{I_m\,\tau_m\cdot\big(1-\gamma_l(t_{pp}-t_{15})\big)\cdot(1+\kappa p_{pp})}\right)\cdot \left(\frac{1}{L_{20,ij}\cdot\big(1+\alpha_{st}(t_{wall}-t_{20})\big)}\right)\cdot \left(\frac{4}{\pi\big(D_{20,ij}\big)^2\big(1+2\alpha_{st}(t_{wall}-t_{20})\big)\left(1+\frac{p_{pp}D_{pp}}{Ew_{pp}}\right)}\right) - 1 \tag{12}$$

The prover is in fact three provers in one. For each orientation j of the switches a deviation e_j is determined using separate timing for the corresponding meter pulses. In this way three independent values of $e_j \pm U$ are obtained. The average is

$$\bar{e} = \frac{1}{3}\sum_{j=1}^{3} e_j \tag{13}$$

The uncertainty of the average consists of two contributions, i.e. the uncertainty of taking the average and the variability of the actual values of e_j expressed by the experimental standard deviation s.

$$U(\bar{e}) = \sqrt{\frac{(2s)^2 + U^2}{3}} \tag{14}$$

In this way the availability of three independent prover volumes leads to a reduction of the uncertainty, i.e. $U(\bar{e}) < U$.

4. Uncertainty contributions

As all models are practically linear the uncertainty analysis can be made in accordance with the classical GUM [4], use of Monte Carlo methods [5] is not necessary.

Apart from the obvious uncertainties of all input parameters there are a number of potential uncertainty sources that require more elaboration. These are:

- Dead volume due to the mass cumulated between reference and MuT.
- Static air inclusion (trapped air).
- Circulating air that is measured by the reference as liquid, but is not measured by the MuT.
- Leak flow.
- Piston velocity and hysteresis
- Influence of dissolved on oil properties

4.1 Dead volume

For both piston proving as well as master metering, the dead volume variation is monitored. By stabilizing the operational process and limiting the pressure and temperature variations during the calibration cycle the dead volume effect can then be treated as an uncertainty source. Furthermore, the influence of dead volume during master metering can be reduced by elongating the time of calibration interval. Both approximations will be discussed below. The deviation change due to the mass stored in the dead volume in the calibration interval is calculated first. Next the uncertainty will be computed associated when dead volume correction is not applied.

Assuming the liquid is homogeneous, the difference in pressure and temperature between the start and the end of the calibration run are the only influence parameters.

The mass cumulated between the reference and the MuT is the left hand side of Eq. (2). The volume between the reference and the MuT is the dead volume V_{dead}, which is constant over time. When we integrate this term over time the dead mass flow rate q_{dead} is

$$q_{dead} = \frac{V_{dead}\,\Delta\bar{\rho}}{\tau_m} \tag{15}$$

Where $\Delta\bar{\rho}$ is the change of the average density in the dead volume between the start and the end of the calibration run. The ratio of q_{dead} and q_m is the error in the observed deviation:

$$\Delta e_{dead} = \frac{q_{dead}}{q_m} = \frac{V_{dead}}{Q_m\tau_m}\cdot\frac{\bar{\rho}_{end}-\bar{\rho}_{start}}{\rho_m} \tag{16}$$

Using Eq. (2, 3) this can be rewritten as

$$\Delta e_{dead} = \frac{V_{dead}}{Q_m\tau_m}\cdot\frac{-\gamma_l(t_{end}-t_{start})+\kappa(p_{end}-p_{start})}{\big(1-\gamma_l(t_m-t_{15})\big)\cdot(1+\kappa p_m)} \tag{17}$$

The difference between t_{end} and t_{start}, and p_{end} and p_{start} are measured during each calibration run. The highest difference in a series of measurement is attributed to the start and the end of the test run for a rough approximation of the effect.

Now the uncertainty associated with Δe_{dead} is

$$u(\Delta e_{dead}) = \frac{I_m V_{dead}}{N_m \tau_m} \cdot \sqrt{\gamma^2 u^2(t_m) + \kappa^2 u^2(p_m)} \qquad (18)$$

Where $\left(1 - \gamma_l(t_m - t_{15})\right) \cdot (1 + \kappa p_m)$ in denominator of Eq. (17) was approximated by 1.

4.2 Static air inclusion

Due to the filling process, a limited amount of air could be trapped in the calibration loop. In order to monitor the amount of air in the system, the amount of liquid is measured which is required to pressurized the system. Because the volume of the system and compressibility of the product are known, the amount of air can be determined.

After pressurizing the loop, most of the air is removed and dissolved in the circulating flow. However a small quantity of air will remain in the test section. Due to small variations in the pressure and temperature in the dead volume these differences may result in a small line pack.

4.3 Circulating air

After circulation small air bubbles may move along with the liquid flow. Some measurement principles will treat these as if they were liquid, other measurement principles will not measure them at all. The difference in the response of the different meter principles is treated as an uncertainty. When bubbles are circulating in closed duct they produce clearly audible noise. However, during operation no moving air bubbles are heard.

Based on tables composed by Battino, Rettich and Tominaga [6] an estimate can be made on the solubility of air and nitrogen in oils. Table 38 (p. 584) shows for heptanes at 300 K an increase of the soluble molar fraction of 0.00117 at 0.101 MPa to 0.0109 at 1 MPa, almost ten times as much. This means that after pressurizing the system and circulating the fluid all free air bubble will dissolve quickly in the oil. This is consistent with the observation that no bubbles are heard.

4.4 Leak flow

The leak flow is determined during the leak flow test. In the leak flow test a blocked section comprising the MuT and the reference is pressurized. After 5 minutes' stabilizing, all pressure and temperature transmitters in the section are measured and recorded for a period of another 5 minutes. The pressure change that is not accounted for by the temperature change is considered the leak flow Q_{leak}. The maximum allowable leak flow is approximately 400 ml/h.

$$\Delta e_{leak} = \frac{Q_{leak}}{Q_m} = \frac{I_m Q_{leak}}{N_m \tau_m} \qquad (19)$$

Assuming a rectangular distribution the associated expanded uncertainty ($k = 2$) is

$$U(\Delta e_{leak}) = \frac{2\sqrt{3}}{3} \cdot \frac{I_m Q_{leak}}{N_m \tau_m} \qquad (20)$$

4.5 Piston velocity and hysteresis

In order to identify the performance and hysteresis of the switches and detection ring, the configuration was tested under various conditions (velocity and distance).

As a result of these test it can be concluded that the velocity of the piston in the operation range does not cause any additional variation in the switch timing mechanism. However, the switching moment is varying as function of distance between the detection ring and the switch and the effect is shown in Figure 3. The maximum variation for the operational range of the switch is $3 \cdot 10^{-4}$ which is treated as a repeatability of the length of the prover section.

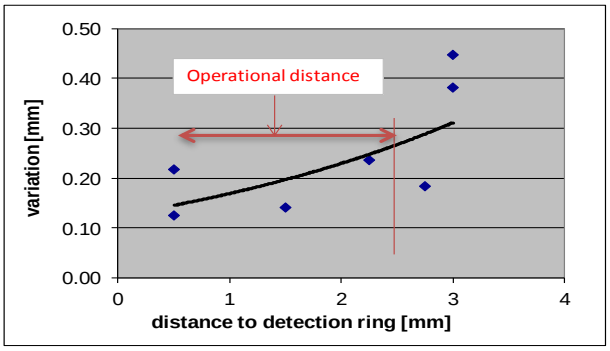

Figure 3: uncertainty source in switching mechanism

4.6 Influence of dissolved air on oil properties

The most important quantity that may be affected is the density. Despite the fact that all trapped air will dissolve completely in oil creating an undersaturated air solution, interstitional air may change the oil density. The initial amount of free air is estimated at 90 L (0.1 kg). This air is dissolved in 40 m³ (30 000 kg). the influence on the density is $3.3 \cdot 10^{-6}$, which is two orders of magnitude smaller than the uncertainty in the density of the oil. Unfortunately, hardly any literature could be found on this effect for oil. For water a relevant study was performed by Harvey et al. [7] who found results for water confirming the order of magnitude on the density change.

In addition PVT simulations were performed [8] on the 100 mm²/s fluid which showed that at 10 bar approximately 10 times the amount of air can be dissolved in oil. This amount is consistent with the values based on [6] mentioned in section 4.3. The influence of the amount of dissolved air as mentioned in the above evaluation led to a relative density change of $1 \cdot 10^{-6}$ and a relative change of kinematic viscosity of $3 \cdot 10^{-5}$, which is an order of magnitude smaller than the other uncertainty sources.

5. Uncertainty results

Table 1 on the last page of this paper gives the full uncertainty analysis of the volume CMC using big piston prover, which includes the above discussed uncertainty sources. Also the averaging procedure of equation (14) is included. The repeatability of a very good flow meter is 0.001% and this value is used to calculate the CMC.

In Tables 2 and 3 the currently accredited CMC values and the CMC values based on the present analysis are listed. The new CMC values are at least a factor 1.4 better than the previous ones. For mass calibrations this is a factor 1.6. The reasons for this improvement is that the calibration process is more stable than initially supposed. The uncertainty of the piston prover was improved by the fact that one pass of the piston results in three independent measurements, which results in a lower uncertainty. The difference between the small prover and the big prover is caused by the smaller scatter between the three parallel sensor runs of the latter.

Table 2: Currently accredited and achievable CMC values for EuroLoop's calibrations of liquid volume flowmeters.

Reference	Accredited volume CMC	Achievable volume CMC
Big Piston Prover	0.020%	0.008%
16" Master meter	0.060%	0.039%
Small Piston Prover	0.020%	0.014%
10" & 6" Master meters	0.060%	0.041%

Table 3: Currently accredited and achievable CMC values for EuroLoop's calibrations of liquid mass flowmeters.

Reference	Accredited mass CMC	Achievable mass CMC
Big Piston Prover	0.040%	0.021%
16" Master meter	0.070%	0.042%
Small Piston Prover	0.040%	0.024%
10" & 6" Master meters	0.070%	0.044%

6. Conclusion

In the preceding pages the liquid volume calibration models were discussed, together with the uncertainty analysis of the EuroLoop Liquid Hydrocarbon Flow Facility. Specific attention was paid to a number of uncertainty sources: dead volume, Static air inclusion (trapped air), circulating air, leak flow, piston velocity and hysteresis and influence of dissolved on oil properties. The analysis shows that improvement of CMCs is possible by a factor of at least 1.4.

The models for mass calibrations could not be included in this paper. The analysis was made in a similar way and here an improvement of the CMCs by a factor 1.6 was realized.

The reason for the improved uncertainties is the process being more stable than initially anticipated. In addition one prover run results in three independent measurement results that allows the corresponding uncertainty be reduced by a factor of $\sqrt{3}$.

Abbreviations and symbols

MM master meter
MuT meter under test·
MMuT mass meter under test
PP piston prover

Symbols

D	internal diameter	[mm]
E	Elasticity modulus	[bar]
e	deviation	[%]
F	Surface of volume V	[m^2]
I	impulse factor	[1/m^3]
N	number of pulses counted during a calibration run	[-]
$\mathbf{n}$	normal vector, perpendicular to F	[-]
p	gauge pressure	[bar]
Q	volume flowrate	[m^3/h]
q	mass flow rate	[kg/h]
t	Celsius temperature	[°C]
V	volume between master meters and MuT	[m^3]
V_{ij}	volume of piston prover section i between switches j	[m^3]
$\mathbf{v}$	fluid velocity vector	[m/s]
w	wall thickness	[mm]
α	linear expansion coefficient	[°C^{-1}]
γ	volume expansion coefficient	[°C^{-1}]
κ	liquid compressibility	[bar^{-1}]
ν	kinematic viscosity	[mm^2/s]
ρ	mass density	[kg/m^3]
τ	time interval corresponding to an integer number of pulses	[s]

Indices

1	at the position of the master meter
2	at the position of the MuT
15	at 15°C
20	at 20°C
i	rank number of the prover volume section
j	rank number corresponding to the orientation of the piston prover switch
l	liquid
M	number of trials in the Monte Carlo simulation
m	indicated by the MuT
mm	indicated by mass meter under test (MMuT)
n	number of parallel master meters
pp	piston prover
q	rank number of the start of the coverage interval
s	standard, i.e. at the master meter
st	steel
V	at the volume between masters and MuT
$wall$	wall conditions

References

[1] RvA (2015): Scope of accreditation for EuroLoop.

[2] Jos van der Grinten, Bart van der Stap and Dick van Driel (2015): Operational experiences with the EuroLoop Hydrocarbon Liquid flow facility, 33rd International North Sea Flow Measurement Workshop, Tønsberg, Norway, 20 - 23 October 2015.

[3] Jos van der Grinten, Bart van der Stap and Pico Brand (2015): Round robin testing for the new EuroLoop liquid flow facility, International Symposium for Fluid Flow Measurement, 14-17 April 2015, Arlington, Virginia, USA

[4] BIPM/IEC/IFCC/ISO/IUPAC/IUPAP/OIML (1993): Guide to the expression of uncertainty in measurement, first edition, ISO 1993

[5] JCGM 101 (2008): Evaluation of measurement data - Supplement 1 to the "Guide to the expression of uncertainty in measurement" - Propagation of distributions using a Monte Carlo method, Guide JCGM 101

[6] Rubin Battino, Timothy R. Rettich and Toshihiro Tominaga (1984): The Solubility of Nitrogen and Air in Liquids, J. Phys. Chem. Ref. Data 13, pp 563-600Erratum: The Solubility of Nitrogen and Air in Liquids [J. Phys. Chem. Ref. Data13, 563 (1984)], J. Phys. Chem. Ref. Data 43, 049901 (2014).

[7] A.H. Harvey, S.G. Kaplan, and J. H. Burnett (2005): Effect of Dissolved Air on the Density and Refractive Index of Water, International Journal of Thermophysics, Vol. 26, No. 5, September 2005.

[8] Bart van der Stap (2016): Analysis of air inclusions in mineral products, *Analyse voor effecten van luchtinsluiting in het product*, Internal report NMi EuroLoop (in Dutch).

Table 1: Uncertainty table for the CMC (k=2) of a volumetric meter under test using the big piston prover. Columns C, D and E represent the three independent measurements of the deviation of the MuT. The sensitivity coefficient c is divided by $1+e_m$ to obtain simpler formulas. The next column G shows the uncertainty contributions, followed by the corresponding uncertainty values (column H). The rightmost column I shows the contribution to the total uncertainty. High uncertainty contributions have a red background, low uncertainties a blue background. The most important contributions result from the diameter calibration of the prover and the temperature measurements. The value at the bottom of the column with the white background is the root sum square addition of all the above contributions. The uncertainty in the adjacent cell with yellow background is the absolute uncertainty of the observed deviation, obtained by multiplying the RSS value in the white cell by $1+e_m$.
All uncertainties in this table are expanded uncertainties represented with a coverage factor k=2.

	A	B	C	D	E	F	G	H	I
1	**Quantity**	**Unit**	**Volume 1**	**Volume 2**	**Volume 3**	**Sensitivity coefficient**	**uncertainty**	**uncertainty**	**uncertainty**
2	**x_i**	**[x_i]**	**x_i [x_i]**	**x_i [x_i]**	**x_i [x_i]**	**c_i / (1+e_m) [1/x_i]**	**sources**	**U(x_i) [x_i]**	**c_i U(x_i) / (1+e_m)**
3	N_m	-	33203	33205	33204	3.0E-05	counting	0.332	1.0E-05
4	κ	bar^{-1}	7.00E-05	7.00E-05	7.00E-05	1.4E+00	API literature	7.0E-06	9.8E-06
5	α	$°C^{-1}$	1.73E-05	1.73E-05	1.73E-05	-2.1E+01	literature	8.7E-07	1.8E-05
6	E	bar	1.93E+06	1.93E+06	1.93E+06	4.6E-11	literature	1.9E+05	8.9E-06
7	WT	m	4.67E-02	4.67E-02	4.67E-02	1.9E-03	calibration	3.3E-03	6.4E-06
8	D	m	1.128	1.128	1.128	-1.8E+00	calibration	2.5E-05	4.5E-05
9	L	m	23.711	23.713	23.711	-4.2E-02	calibration	4.5E-04	1.9E-05
10						-4.2E-02	repeatability	3.0E-04	1.3E-05
11	p_m	bar	8.550	8.550	8.550	7.0E-05	calibration	0.010	7.0E-07
12						7.0E-05	repeatability	0.020	1.4E-06
13						7.0E-05	drift	0.020	1.4E-06
14	p_{pp}	bar	7.154	7.154	7.154	-8.2E-05	calibration	0.010	8.2E-07
15						-8.2E-05	repeatability	0.020	1.6E-06
16						-8.2E-05	drift	0.020	1.6E-06
17	τ_m	s	22.207	22.208	22.208	-4.5E-02	calibration	3.0E-05	1.4E-06
18						-4.5E-02	repeatability	4.3E-05	1.9E-06
19						-4.5E-02	drift	3.0E-05	1.4E-06
20	τ_{pp}	s	22.207	22.208	22.208	4.5E-02	calibration	3.0E-05	1.4E-06
21						4.5E-02	repeatability	4.3E-05	1.9E-06
22						4.5E-02	drift	3.0E-05	1.4E-06
23	γ	$°C^{-1}$	7.34E-04	7.34E-04	7.34E-04	2.5E-01	calibration	1.8E-07	4.6E-08
24						2.5E-01	interpolation	1.7E-05	4.2E-06
25	t_m	°C	27.354	27.354	27.354	7.3E-04	calibration	0.040	2.9E-05
26						7.3E-04	repeatability	0.050	3.6E-05
27						7.3E-04	drift	0.050	3.6E-05
28	t_{pp}	°C	27.101	27.101	27.101	-7.3E-04	calibration	0.040	2.9E-05
29						-7.3E-04	repeatability	0.050	3.6E-05
30						-7.3E-04	drift	0.050	3.6E-05
31	t_w	°C	27.101	27.101	27.101	-5.2E-05	calibration	0.2	1.0E-05
32	q_{leak}	m^3/h	0	0	0	3.0E-04	leak flow	0.0018	5.5E-07
33	q_{leak_piston}	m^3/h	0	0	0	3.0E-04	leak flow piston	0.0005	1.4E-07
34	q_{air_incl}	m^3/h	0	0	0	3.0E-04	static air inclusions	2.1E-07	6.3E-11
35						3.0E-04	flow air bubbles	9.1E-03	2.7E-06
36	t_{15}	°C	15	15	15	0	constant	0	0
37	t_{20}	°C	20	20	20	0	constant	0	0
38	I_m	$pulse/m^3$	1400	1400	1400	0	constant	0	0
39	e_{dead_volume}	-	-0.009%	-0.009%	-0.009%	1.0E+00	dead volume	2.2E-05	2.2E-05
40	$e_{m,i}$	-	0.057%	0.054%	0.063%	1.0E+00	CMC repeatability	0.001%	1.0E-05
41									
42	**$e_{m,i}$**	-	**0.057%**	**0.054%**	**0.063%**			**0.0105%**	1.0E-04
43									
44	e_m						repeatability	0.0052%	
45							averaging unc.	0.0060%	
46	**e_m**	-	**0.058%**				**CMC (k=2)**	**0.0080%**	